Materials Research Proceedings 54 (2025) 780-791 https://doi.org/10.21741/9781644903599-84

Effect of material characterization via torsion tests on the accuracy of FEM simulations in the extrusion process

Sara Di Donato[1,a *], Riccardo Pelaccia[2,b], Marco Negozio[3,c], Nicola Lai[1,d], Mohamad El Mehtedi[4,e], Barbara Reggiani[2,5,f] and Lorenzo Donati[1,g]

[1]University of Bologna - DIN Department of Industrial Engineering, Viale Risorgimento 2, 40136, Bologna, Italy

[2]University of Modena and Reggio Emilia - DISMI Department of Sciences and Methods for Engineering, Via Amendola 2, 42122, Reggio Emilia, Italy

[3]University of Parma - DISTI Department for Industrial Systems and Technologies, Parco Area delle Scienze, 181/A, 43124 Parma, Italy

[4]University of Cagliari – DIMCM Department of Mechanical, Chemical and Materials Engineering, Via Marengo 2, 09123 Cagliari, Italy

[5]University of Modena and Reggio Emilia - InterMech - MO.RE, Piazzale Europa 1, Reggio Emilia 42124, Italy

[a]sara.didonato2@unibo.it, [b]riccardo.pelaccia@unimore.it, [c]marco.negozio@unipr.it, [d]nicola.lai5@unibo.it, [e]m.elmehtedi@unica.it, [f]barbara.reggiani@unimore.it, [g]l.donati@unibo.it

Keywords: Hot Torsion Test, Flow Stress, Material Characterization, Aluminum Extrusion, FEM Simulation

Abstract. The Finite Elment Method codes are nowadays potent and useful tools for advancing the design and optimization of metal forming processes. This is particularly evident in sectors such as aluminum extrusion, where FEM contributes to both process enhancement and tool development, mitigating the high costs and time demands of experimental trials. However, accurate and reliable simulations require precise material flow stress modeling. In this context, the hot torsion test is considered the most suitable for material characterization as it allows for achieving the high strain levels typical of the extrusion process while maintaining stable temperature and strain rate conditions during testing. This work presents the characterization via torsion tests of four distinct alloys, all classified within the AA6082 series, obtained from different casting batches. The resulting data were subsequently employed as input for numerical simulations of an industrial extrusion process and compared with experimental results to assess the impact of flow stress modeling on the accuracy and reliability of the simulations.

Introduction

Over the years, FEM codes have been increasingly used in the industry and manufacturing sector thanks to their continuous development, robustness, and reliability in simulation results. Specifically, in the case of the extrusion and rolling processes, numerical simulations have been employed to improve the process parameters and die design [1]. The codes allow the optimization of different aspects and requirements, such as material flow balancing, product quality, and reducing scraps, thereby minimizing the time and costs associated with experimental trials [2–4]. In recent years, different numerical approaches and methodologies have been proposed for the prediction of charge welds, surface recrystallization, and grain structure during the extrusion of AA6XXX alloys [5,6], as well as for optimizing nitrogen cooling in extrusion dies and investigating deformation texture [7–10]. A fundamental aspect of obtaining accurate simulations is the material card provided to the FEM software to characterize the material's response during deformation and manufacturing processes. It is necessary to provide the code with a precise flow

stress model. Therefore, appropriate characterization tests are required to achieve high deformation values typical of the extrusion and rolling processes maintaining constant temperature and strain rates. In this context, the most suitable test is considered the hot torsion test, where a solid or tubular specimen is twisted by a torque applied around its axis at a constant angular velocity [11–13]. Since the solid specimen under torsion does not change its geometry during deformation, extended strain values are achieved, overcoming the limits of the high-temperature tensile and compression tests where the flow curves are usually limited respectively to 0.2-0.3 and 0.8-1 of true strain [14,15].

This study aims to present and compare the plastic behavior of various aluminum alloys classified as AA6082, sourced from different batches. It also investigates the influence of material flow stress modeling on the accuracy of numerical simulations by comparing predicted outcomes with experimental data from an industrial extrusion case study. Although the four alloys considered in this study are all classified as AA6082 and were homogenized under the same temper condition (Condition O), small variations in chemical composition within the standard specifications could contribute to the observed differences in flow behavior. Furthermore, different suppliers of alloy might use different homogenization cycles, and potential minor variations in the homogenization cycle (e.g., ramp rate, soaking time, or cooling rate) could also play a role in influencing the microstructural state and, consequently, the flow stress behavior. In this context, the torsion test demonstrates its potential not only as a tool for investigating plastic behavior but also as a quality control method for identifying subtle differences in incoming materials that might not be apparent through standard classification. The hot torsions tests were conducted using the equipment available at the University of Bologna, in the DIN-Department of Industrial Engineering, with three different strain rate conditions: 0.1 s^{-1}, 1 s^{-1}, and 10 s^{-1}, and three different temperatures: 450°C, 500°C, and 550°C. Regarding the extrusions, the case study considered for the experimental-numerical comparison was taken from the Extrusion Benchmark 2023 presented at the Aluminium2000 International Conference on Extrusion and Benchmark [16]. Subsequently, extrusion numerical simulations were modeled using the commercial software QForm UK®.

Materials and method

Torsion Test. The hot torsion tests were performed using aluminum solid cylindrical specimens, with a gauge length and a diameter of 10 mm, as shown in Fig. 1a. This type of geometry allows for easier temperature control along the specimen's section and can withstand higher torque and greater fracture strain compared to thin-walled tubular specimens [15]. Also, the specimen design includes a hole with a diameter of 3 mm and a length of 52.5 mm, allowing a thermocouple to be inserted inside it to measure the specimen's temperature during the test, near the gauge section. Before torsion, the samples were heated using an induction copper solenoid, with a ramp rate of 1°C/s and a 5-minute holding period to ensure homogeneous temperature distribution throughout the gage length, as shown in Fig. 1b. The thermocouple enables the temperature to be maintained constant throughout the test using a PID controller.

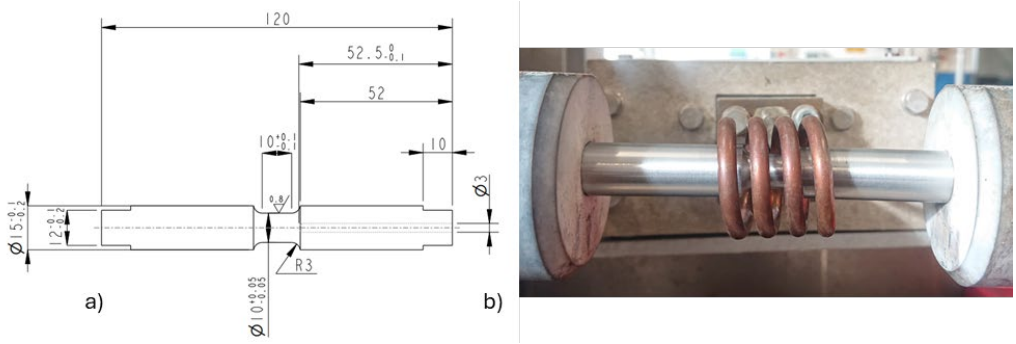

Figure 1 – a) Geometry of the solid bar specimen, with dimensions (in mm); b) Pictures of an AA6082 sample during the hot torsion test performed at the University of Bologna - Department of Industrial Engineering.

During the torsion test, the outputs provided by the machine refer to the torque [N·mm] and the torsion angle in radians applied to the specimen. Subsequently, the Fields-Backofen model [17] is used to calculate the shear strain γ and the corresponding shear stress τ [MPa], allowing for the consideration of strain, stress, and strain rate corresponding to the outer diameter of the torsion specimen, as expressed in Eq. 1, Eq. 2, and Eq. 3.

$$\gamma = \frac{R\,\theta}{L}\,, \tag{1}$$

$$\dot{\gamma} = \frac{R\,\dot{\theta}}{L}\,, \tag{2}$$

$$\tau = \frac{M}{2\,\pi\,R^3}(3 + n + m)\,, \tag{3}$$

where M is the torque moment expressed in N·mm, L is the length of the gauge section of the specimen (10 mm) and R is the radius (5 mm), as indicated in Fig. 2. The term n is the strain hardening coefficient (instantaneous slope of logM vs. logθ as expressed in Eq. 4 and m is the strain rate sensitivity coefficient (slope of logM vs. log$\dot{\theta}$ at fixed values of θ as in Eq. 5.

$$n = \left.\frac{\partial \log M}{\partial \log \theta}\right|_{\dot{\theta}}\,, \tag{4}$$

$$m = \left.\frac{\partial \log M}{\partial \log \dot{\theta}}\right|_{\theta}\,. \tag{5}$$

Numerous studies have demonstrated that the strain hardening and strain rate sensitivity coefficients have negligible effects on aluminum alloys when calculating stress, as their influence on the material's behavior at high temperatures is minimal [12,15,18]. Therefore, in this study, the coefficients m and n were neglected, obtaining the equivalent Von Mises stress and strain as expressed in Eq. 6 and Eq. 7.

$$\bar{\sigma} = \frac{M\,3\sqrt{3}}{2\,\pi\,R^3}\ , \tag{6}$$

$$\bar{\varepsilon} = \frac{\gamma}{\sqrt{3}}\ . \tag{7}$$

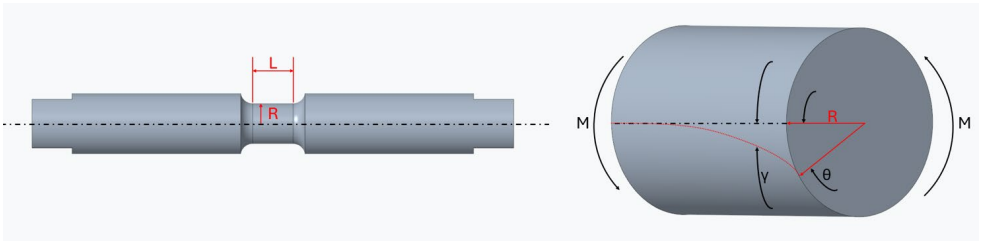

Figure 2 – Scheme of the specimen, highlighting the shear strain occurring along the gauge length.

Extrusion numerical simulation. The industrial case study involved the extrusion of three tube-shaped profiles, with an outer diameter of 40 mm and a thickness of 4 mm. The die design presented three openings with different cylindrical or conical ports, bearing lengths, and radii to achieve varied metal flow within the extruded profiles. During the process, several parameters were monitored, including the profile exit temperature, exit speed, and extrusion force. The key process specifications are summarized in Table 1, and further details can be found in references [2,16].

Table 1 – Extrusion process parameters

Process Parameter	Value
Profile alloy	AA6082
Billet diameter [mm]	279
Container diameter [mm]	286
Billet length [mm]	680 [mm]
Billet rest [mm]	30 [mm]
Ram speed [mm/s]	4.4 [mm/s]
Max press load [MN]	40[MN]
Ram/Container Temperature [°C]	350 / (390-425)
Pre-heating Billet/Die Temperature [°C]	440 (no taper) / 480

The extrusion numerical model was implemented using the commercial software QForm UK® through the Arbitrary-Lagrangian-Eulerian module designed to simulate industrial extrusion processes, as shown in Fig. 3. The simulation was prepared in accordance with guidelines derived from prior validation studies that compared the results of extrusion simulations with experimental data [10,11]. For the design of 3D geometries, the Qshape internal module was used to generate the volumetric meshes of the tools and workpiece, the details are summarized in Table 2. Regarding the billet, the material flow stress values were set in tabular form based on experimental results obtained from torsion tests, while the physical and thermal properties were set according to the AA6082 standard database as listed in Table 3. As for the tools - die, ram, and container - the mechanical, physical, and thermal properties were set to the default values for H13 steel available in the QForm database. Finally, the Levanov model was selected to define the friction conditions between the workpiece and the tools, with a friction factor of 1, a Levanov coefficient of 1.25 and a Heat transfer coefficient of 3000 [W/(m2·K)].

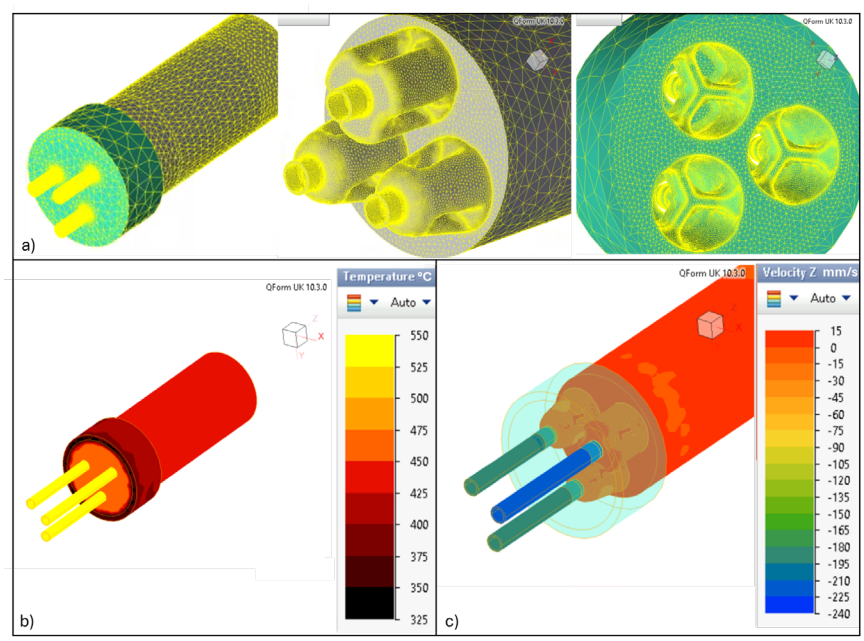

Figure 3 – Simulation of the extrusion process with Qform Extrusion UK®. a) workpiece and tools mesh; b) temperature distribution in °C; c) velocity in z-direction in mm/sec.

Table 2 – Mesh parameters.

Object	Nodes on surface	Internal nodes	Total nodes	Surface elements	Volumetric elements
Workpiece	45977	114651	160628	91986	843450
Die set	45772	133972	179744	91576	962155
Total	91749	248623	340372	183562	1805605

Table 3 – Material parameters for the AA6082 alloy.

Material Properties	AA6082
Density [kg/m3]	2608
Specific heat [J/(kg·K)]	1017
Thermal conductivity [W/(m·K)]	217
Thermal expansion [1/°C]	2.73e-5
Young's modulus [MPa]	46000
Poisson's ratio	0.36

Results and discussion

Hot torsion tests on Aluminum alloys. Hot torsion tests were performed on specimens extracted from four different aluminum batches, all classified as AA6082 and industrially homogenized to an O condition. The batches were labeled Alloy 1, Alloy 2, Alloy 3, and Alloy 4.

Materials Research Proceedings 54 (2025) 780-791 https://doi.org/10.21741/9781644903599-84

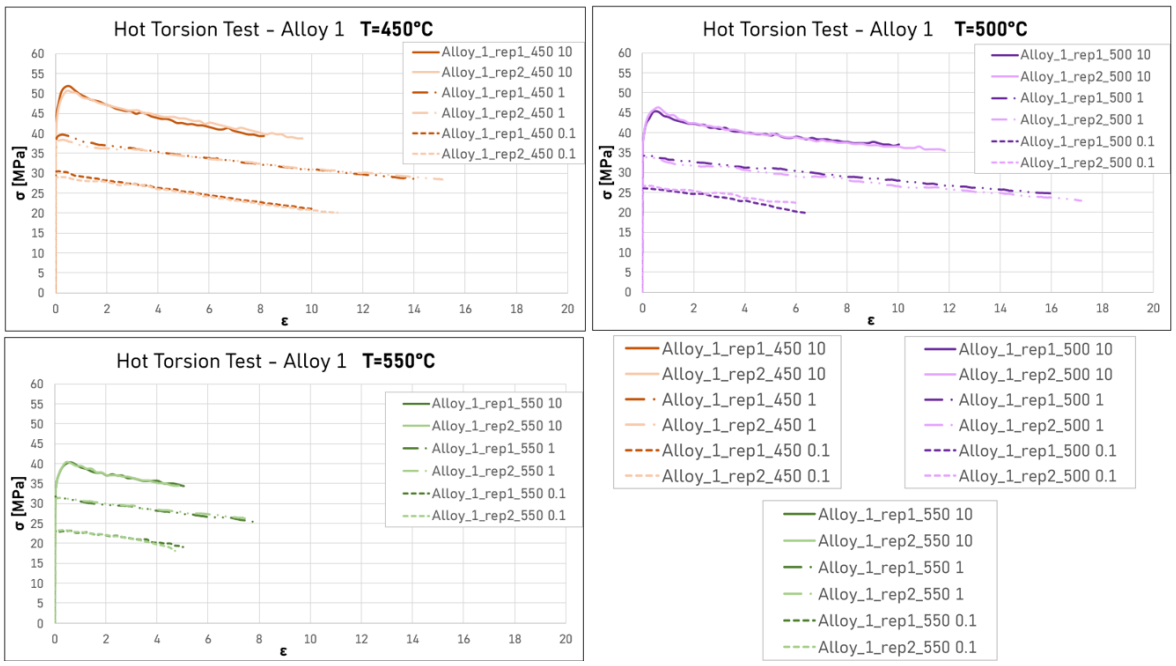

Figure 4 – Experimental σ-ε curves of Alloy 1. Two trials for each condition: three temperatures, 450°C, 500°C, 550°C, and three strain rates, 0.1 s^{-1}, 1 s^{-1}, and 10 s^{-1}.

The tests were conducted at three different strain rates (0.1 s^{-1}, 1 s^{-1}, and 10 s^{-1}) and at three temperatures (450°C, 500°C, and 550°C). For each condition, at least two tests were performed to assess repeatability. The graphs in Fig. 4 present the experimental results for Alloy 1, showing equivalent stress [MPa] vs. equivalent strain. In the graphs, flow stress curves are grouped by temperature, with red lines representing tests at 10 s^{-1}, green lines at 1 s^{-1}, and blue lines at 0.1 s^{-1}. The results confirm the high repeatability of the tests. During the torsion phase, the temperature is maintained constant using a PID controller that regulates induction heating, with a tolerance of ±3°C due to the heat generated during deformation and thermal exchange between the specimen and the grips, as shown in Fig. 5.

Fig. 6 presents the results of the torsion tests performed on the four alloys. In each graph, the orange curves represent tests conducted at a strain rate of 10 s^{-1}, the green curves at 1 s^{-1}, and the blue curves at 0.1 s^{-1}, while the different line styles denote the various temperatures. The flow stress curves reveal the typical behavior observed in many aluminum alloys, characterized by a peak at small strains followed by a softening phase. The tests were stopped after the specimens were fractured. Specifically, the specimens of Alloy 1 tested at 550°C reached strain values between 4.5 and 8, whereas they exhibited greater ductility at temperatures of 450°C and 500°C, achieving strain values between 14 and 16 during tests conducted at a strain rate of 1 s^{-1}. Alloy 1 proved to be the most resistant, showing stress values approximately 6-10 MPa higher than the other alloys for each strain rate condition. Additionally, Alloy 3 exhibited a more pronounced softening mechanism compared to the other alloys, with stress values decreasing significantly as strain increases. Finally, Alloy 4 demonstrated lower ductility compared to the other alloys, with all specimens failing at strain values between 5 and 6.

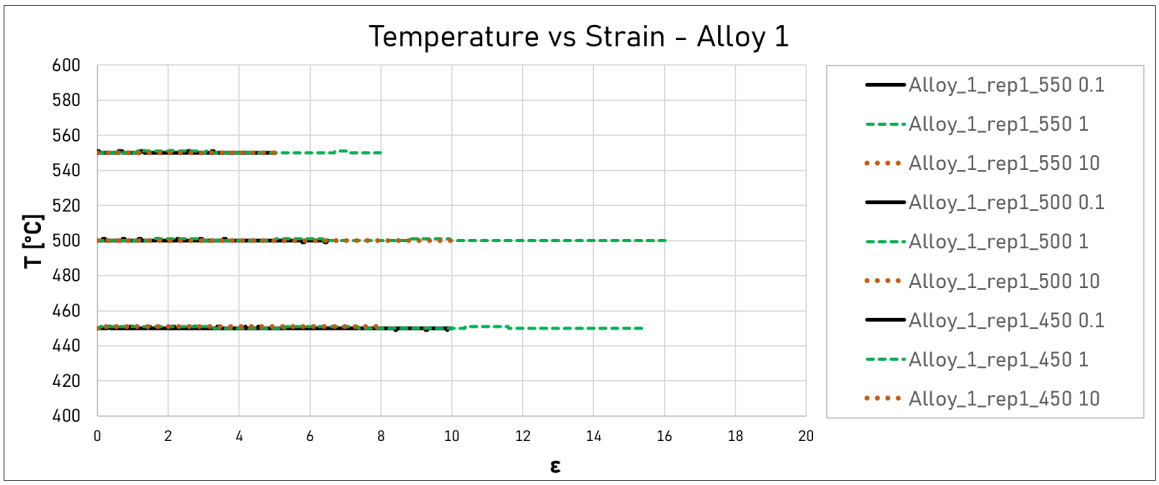

Figure 5 – Temperature control during the tests on Alloy 1.

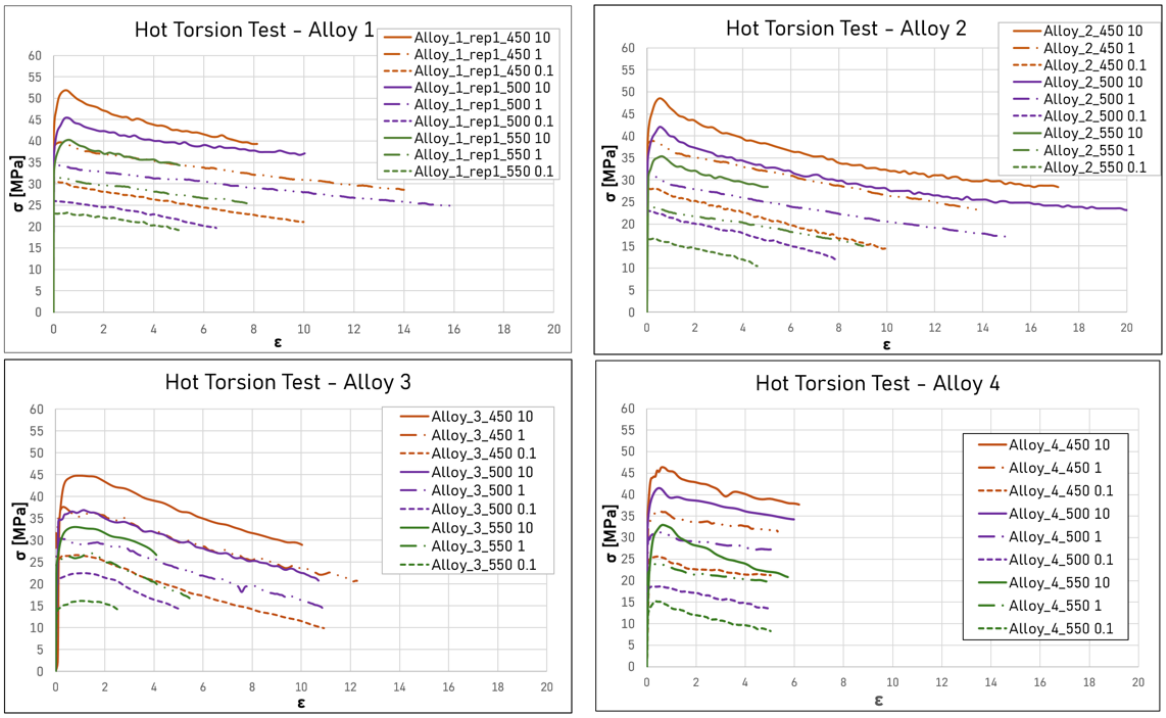

Figure 6 – Experimental σ-ε curves of Alloys 1, 2, 3 and 4.

Extrusion experimental numerical comparison. Four different numerical simulations of the extrusion case study were run. In each simulation, all model and tool parameters were kept constant, while only the material's flow stress was varied. The flow stress data used as input corresponded to the four alloys and were derived from the torsion test results. The output values from the numerical simulation, such as extrusion load, profile speeds, and profile exit temperature, were compared with the experimental data collected during the extrusion campaign presented in [16], as shown in Fig. 7. The comparison results are presented in Fig. 8, Fig. 9, and Fig. 10. It is important to highlight that only for Alloy 1 the extrusion was carried out from the casting batch, and experimental data were collected, whereas for alloys 2, 3, and 4 the extrusions were exclusively simulated.

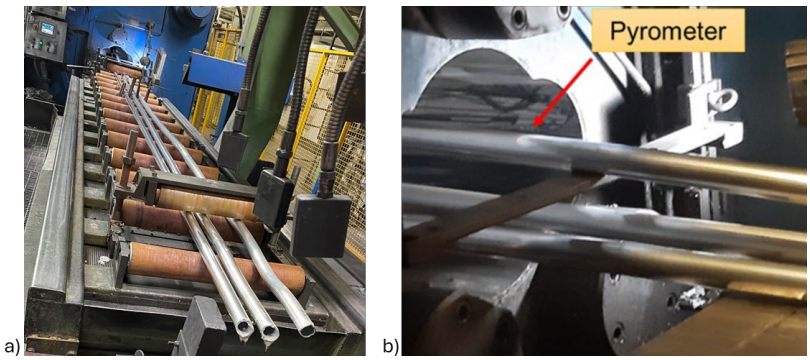

Figure 7 – Photographs of the experimental extrusion campaign [16]: a) Extrusion of the three profiles; b) Detail of the temperature measurement using a non-contact pyrometer.

Fig. 8 shows the relationship between the extrusion load [MN] and the piston stroke [mm]. The experimental peak value was 36 MN, with a statistical distribution of 1.35%. As the ram stroke progressed, the press load decreased due to the reduction of material in the container and diminishing friction forces. The numerical peak results were 35 MN in the simulation performed using the flow stress of Alloy 1, with an error of approximately 2% compared to the experimental data. For the other simulations, peak load values were 32 MN for Alloy 2, 28 MN for Alloy 3, and 30 MN for Alloy 4, with errors ranging between 10% and 21%. The results demonstrate, on one hand, the relatively limited scattering in flow stress values across different casting batches (Alloy 1 vs. Alloy 2 vs. Alloy 3 vs. Alloy 4), and on the other hand, the significant impact that minor differences in values have on load-stroke predictions using FEM.

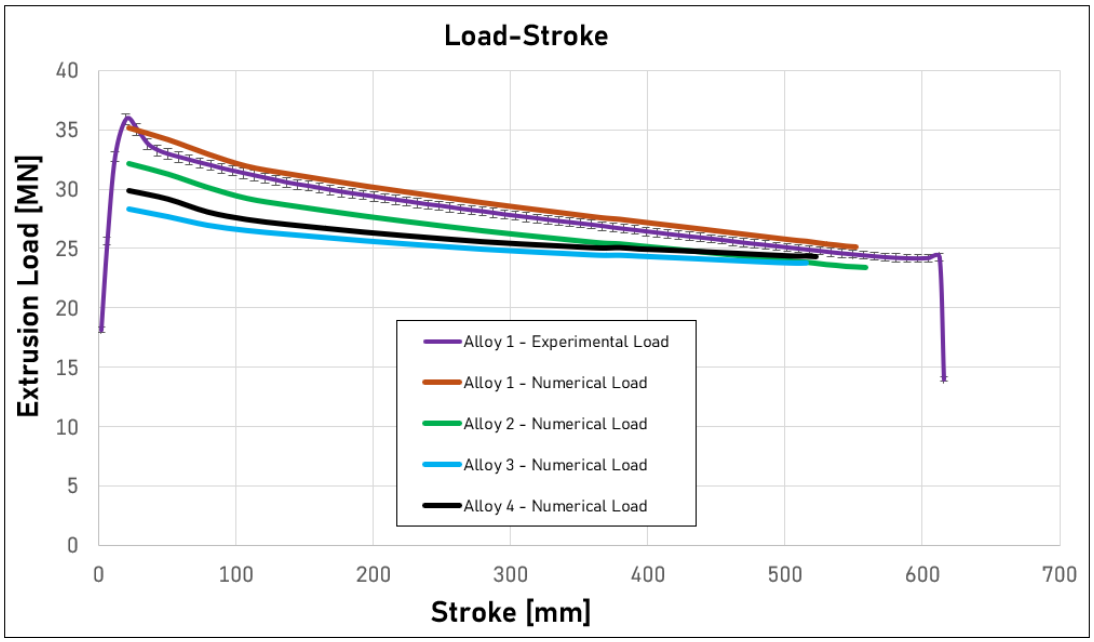

Figure 8 – Comparison between the experimental extrusion load with numerical results obtained using the flow stress data of Alloy 1, Alloy 2, Alloy 3 and Alloy 4.

Moving on to the extrusion exit speed, the three different profiles exhibited differences due to the varying geometry of the ports and bearings. Before the use of the puller, Profile 2 had a velocity 50% higher than that of the other two profiles, and even with the tensile puller force of 3500 N, it continued to exhibit a higher velocity. Fig. 9 shows that the speed of profiles 1 and 3, controlled by the puller, was 195 mm/s, while the speed of Profile 2 averaged 225 mm/s, calculated by analyzing the difference in the extruded lengths at the end of the extrusion process. In the simulations, to replicate the same conditions as the experimental extrusion process, the speeds of

profiles 1 and 3 were imposed by a velocity boundary condition, while Profile 2 was allowed to flow freely through the die. From the numerical results, it was found that the velocity is not significantly influenced by the material flow stress, with simulated Profile 2 velocity values showing errors of less than 1%, with respect to the experimental data for all cases.

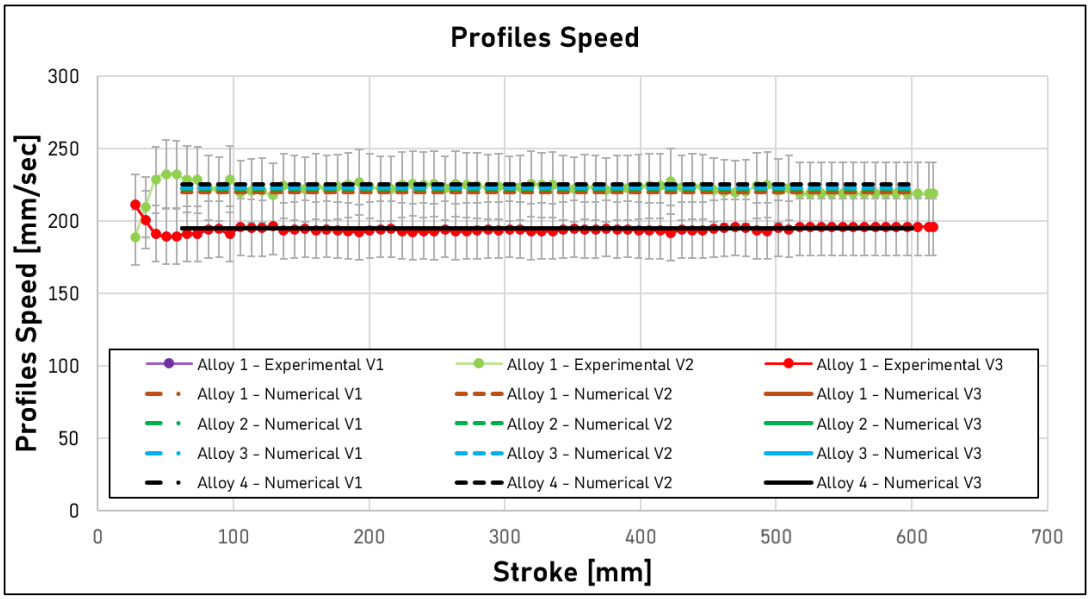

Figure 9 – Numerical-Experimental comparison of the profile's exit speeds.

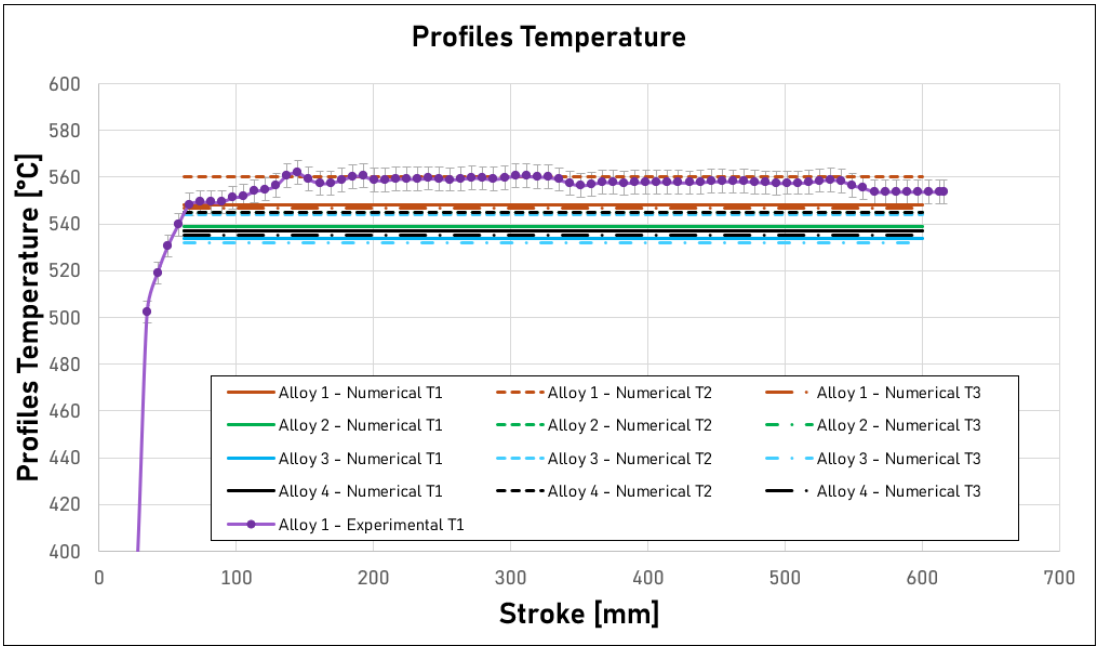

Figure 10 – Comparison between the experimental profiles' temperature and numerical ones

Regarding the experimental temperatures of the profiles, a non-contact pyrometer was used to monitor only the temperature of Profile 1 at a distance of 1500mm from the bolster surface, as shown in Fig. 7. Fig. 10 compares the temperature values predicted by the simulations with the temperature measured experimentally on Profile 1 with a standard deviation of 0.9%. Among the four different alloys, the lowest temperatures were recorded for Profile 1, with an error of about 1.5% for Alloy 1, 3% for Alloy 2, 4% for Alloy 3, and 3.5% for Alloy 4.

Conclusion

In this study, the plastic behavior of four different homogenized billets of AA6082 alloy was characterized through hot torsion tests conducted at the University of Bologna - Department of Industrial Engineering. The tests were performed at three strain rates: 0.1 s^{-1}, 1 s^{-1}, and 10 s^{-1}, and three different temperatures: 450°C, 500°C, and 550°C. The flow stress curves of each alloy, designated as Alloy 1, Alloy 2, Alloy 3, and Alloy 4, were provided. The results revealed differences in strength and ductility among the alloys, despite all being classified as AA6082. Alloy 1 exhibits slightly higher resistance compared to the other alloys, reaching larger stress values under all test conditions. Alloy 3 demonstrated a more pronounced softening behavior than the other three alloys, while Alloy 4 showed the lowest ductility with strain values ranging between 4 and 6. The alloys' flow stress curves were subsequently used as input data for FEM simulations of an industrial extrusion process performed using QForm UK®. The numerical results were compared with experimental data collected during the extrusion of three hollow tubes using Alloy 1. The experimental-numerical comparison allowed for determining the accuracy of the simulations in terms of extrusion load, extrusion speed, and profile temperature. The highest accuracy was achieved with alloy 1, with an error of 2% on the extrusion load peak and 1.5% on the temperature, while for the other alloys, the errors ranged between 10% and 21% for the load peak and between 3% and 4% for the temperature, while for the extrusion speed, all four alloys exhibited an error of less than 1%. The results highlight the importance of proper experimental characterization of the flow stress of materials to ensure good reliability of the data obtained from numerical simulations.

Fundings

This study is funded by the Italian Ministry of University and Research, PNRR, Mission 4, Component 2, Investment line 1.1—Call for tender No. 104 published on 2.2.2022 by the Italian Ministry of University and Research (MUR), funded by the European Union—NextGenerationEU–Project Title: "SCULPTROL—SCULPTuring by ROLling for multi-material bonding"— COD. PROGETTO 2022NMJC38 - CUP: J53D23002300006—Grant Assignment Decree No 961 adopted on 30 June 2023 by the Italian Ministry of Ministry of University and Research (MUR).

Acknowledgements

Authors acknowledge the financial support under the Italian Ministry of University and Research, PNRR, Mission 4, Component 2, Investment line 1.1—Call for tender No. 104 published on 2.2.2022 by the Italian Ministry of University and Research (MUR), funded by the European Union—NextGenerationEU–Project Title: "SCULPTROL—SCULPTuring by ROLling for multi-material bonding"— COD. PROGETTO 2022NMJC38 - CUP: J53D23002300006—Grant Assignment Decree No 961 adopted on 30 June 2023 by the Italian Ministry of Ministry of University and Research (MUR). Nicola Lai acknowledges the financial support under the National Recovery and Resilience Plan (NRRP), Mission 4, Component 2, Investment 1.1, Call for tender No. 104 published on 2.2.2022 by the Italian Ministry of University and Research (MUR), funded by the European Union – NextGenerationEU– Project Title "3D Structured interfaces for improved strength of HYbrid Metal-Composites joints with self-sensing capabilities – 3DSHYMCO" – CUP J53D23002470006 - Grant Assignment Decree No. 2022WFK8WT adopted on 30/06/2023 by the Italian Ministry of Ministry of University and Research (MUR).

References

[1] L. Donati, B. Reggiani, R. Pelaccia, M. Negozio, S. Di Donato, Advancements in extrusion and drawing: a review of the contributes by the ESAFORM community, Int J Mater Form 15 (2022) 41. https://doi.org/10.1007/s12289-022-01664-w

[2] R. Pelaccia, M. Negozio, S. Di Donato, B. Reggiani, L. Donati, Numerical simulation of the extrusion process with different FEM code approaches: analysis of thermal field, profile speed, defects evolution, and microstructure of hollow tubes, in: 2024: pp. 771–780. https://doi.org/10.21741/9781644903131-85

[3] L. Raimondi, F. Bernardi, Advanced hybrid laminates: elastomer integration for optimized mechanical properties, Int J Adv Manuf Technol 136 (2025) 3177–3195. https://doi.org/10.1007/s00170-025-15023-x

[4] F. Bernardi, A. Sensini, L. Raimondi, L. Donati, On the infiltration of cellular solids by sheet molding compound: process simulation and experimental validation, Int J Adv Manuf Technol 133 (2024) 3745–3755. https://doi.org/10.1007/s00170-024-13977-y

[5] M. Negozio, A. Segatori, R. Pelaccia, B. Reggiani, S. Di Donato, L. Donati, Modeling of recrystallization behaviour of AA6xxx aluminum alloy during extrusion process, Transactions of Nonferrous Metals Society of China 34 (2024) 3170–3184. https://doi.org/10.1016/S1003-6326(24)66600-8

[6] M. Negozio, R. Pelaccia, L. Donati, B. Reggiani, S. Di Donato, Microstructure Evolution and FEM Prediction on AA6XXX Alloys, Key Engineering Materials 987 (2024) 3–10. https://doi.org/doi:10.4028/p-qO8WAd

[7] K. Zhang, K. Marthinsen, B. Holmedal, T. Aukrust, A. Segatori, Through thickness variations of deformation texture in round profile extrusions of 6063-type aluminium alloy: Experiments, FEM and crystal plasticity modelling, Materials Science and Engineering: A 722 (2018) 20–29. https://doi.org/10.1016/j.msea.2018.02.081

[8] S. Di Donato, R. Pelaccia, M. Negozio, Phase Field Method for the Assessment of the New-Old Billet Material Interaction during Continuous Extrusion Using COMSOL Multiphysics, J. of Materi Eng and Perform (2024). https://doi.org/10.1007/s11665-024-10013-8

[9] R. Pelaccia, M. Negozio, S.D. Donato, L. Donati, B. Reggiani, Recent Trends in Nitrogen Cooling Modelling of Extrusion Dies, Key Engineering Materials 987 (2024) 11–22. https://doi.org/doi:10.4028/p-Q0NDkB

[10] M. Negozio, R. Pelaccia, L. Donati, B. Reggiani, S. Di Donato, Validation of charge welds and skin contamination FEM predictions in the extrusion of a AA6082 aluminum alloy, in: 2023: pp. 86–93. https://doi.org/10.21741/9781644902714-11

[11] J.D. Bressan, R.K. Unfer, Construction and validation tests of a torsion test machine, Journal of Materials Processing Technology 179 (2006) 23–29. https://doi.org/10.1016/j.jmatprotec.2006.03.099

[12] M. El Mehtedi, S. Spigarelli, F. Gabrielli, L. Donati, Comparison Study of Constitutive Models in Predicting the Hot Deformation Behavior of AA6060 and AA6063 Aluminium Alloys, Materials Today: Proceedings 2 (2015) 4732–4739. https://doi.org/10.1016/j.matpr.2015.10.006

[13] S. Di Donato, R. Pelaccia, M. Negozio, M.E. Mehtedi, B. Reggiani, L. Donati, Hot Torsion Tests of AA6082 Alloy, Key Engineering Materials 988 (2024) 21–29. https://doi.org/10.4028/p-5c0LIi

[14] S.C. Shrivastava, J.J. Jonas, G. Canova, Equivalent strain in large deformation torsion testing : Theoretical and practical considerations, Journal of the Mechanics and Physics of Solids 30 (1982) 75–90. https://doi.org/10.1016/0022-5096(82)90014-X

[15] G.E. Dieter, H.A. Kuhn, S.L. Semiatin, eds., Handbook of workability and process design, ASM International, Materials Park, Ohio, 2003.

[16] R. Pelaccia, M. Negozio, S. Di Donato, B. Reggiani, L. Donati, Extrusion Benchmark 2023: Effect of Die Design on Profile Speed, Seam Weld Quality and Microstructure of Hollow Tubes, Key Engineering Materials 988 (2024) 47–62. https://doi.org/10.4028/p-gNXRC5

[17] Jr. Fields, W.A. Backofen, Determination of strain-hardening characteristics by torsion testing, Proc. Am. Soc. Test. Mater. 57 (1957) 1259–1272.

[18] B. Verlinden, A. Suhadi, L. Delaey, A generalized constitutive equation for an AA6060 aluminium alloy, Scripta Metallurgica et Materialia 28 (1993) 1441–1446. https://doi.org/10.1016/0956-716X(93)90496-F